A theory of wind-driven circulation. I. Mid-ocean gyres

by Peter B. Rhines[1] and William R. Young[1,2]

ABSTRACT

A theory of the wind-driven ocean circulation is presented in which the key feature is strong deformation of interior density layers and consequent production of closed geostrophic-contours by the flow itself. The constraint imposed on the subsurface flow by the imposition of a no flux condition where a geostrophic contour strikes a coastal boundary is thus removed. Within regions where the geostrophic contours close the potential vorticity is uniform. This expulsion of gradients of q to the rim of the wind-driven gyre relies on a lateral eddy flux of potential vorticity or equivalently (for gyre-scale mean flows) a vertical transport of momentum by eddy 'form drag'. The same result can also be obtained by invoking interfacial drag proportional to the velocity difference between layers as a specific model of form drag.

The circulation models constructed here are intended as the simplest possible theoretical application of the potential vorticity homogenization results previously given by Rhines and Young (1982). There it was argued that potential vorticity homogenization amounts to a singular perturbation with respect to eddy processes; infinitesmal eddy fluxes can produce a finite mean flow in a region where the geostrophic contours close. In this article we show how the extent of the homogenized region, and the three-dimensional structure of the mean flow within it, follow directly by requiring the potential vorticity to be uniform.

The theory exhibits the poleward migration of gyre centers with depth, and an abrupt poleward gyre boundary familiar to observations of the major subtropical current systems. The Sverdrup constraint on the vertically integrated velocity applies throughout. The solutions develop discontinuities which are important to their maintenance.

Comparisons are made with classical advective thermocline theory. The major difference in philosophy is that we consider the development of the wind-driven circulation on a known basic density profile, over a 'fast' time-scale, with evolution of the basic stratification left to a 'slow' time-scale. The solutions given here rely on vertical eddy momentum transport (which is also a lateral potential vorticity transport), usually ignored in the classical theory. The results are unique and almost independent of details of the eddy processes. The lateral eddy fluxes of potential vorticity become very weak once the circulation is spun up, yet they are essential to its creation and existence. The solution near outcropping regions, where fluid is injected from the mixed layer, is not calculated here. Coastal boundaries are omitted from this study to simplify the development. The indications are that western boundary currents, though important to the vertically integrated dynamics, play a weak role on the 'interior' density surfaces. They are treated in a succeeding paper (Young and Rhines, 1982).

1. Woods Hole Oceanographic Institution, Woods Hole, Massachusetts, 02543, U.S.A.
2. Present address: Scripps Institution of Oceanography, A005, La Jolla, California, 92093, U.S.A.

1. Introduction

The ocean circulation posed as a theoretical problem is so complex that it is necessary to look at parts of it in isolation. In this spirit valuable progress has been made with steady homogeneous-fluid wind-driven circulations, with idealized meridional circulations driven by buoyancy forcing, and with the spin-up of wind circulation from rest. Unfortunately most of these investigations, excepting that known as thermocline theory and certain boundary layer theories, imagine the basic potential-vorticity field to be dominated by β, the northward gradient of Coriolis frequency. Rhines and Holland (1979) discuss the way in which flow may reshape the potential vorticity, q, so that flow paths q = const. in quiet regions connect with surface boundary conditions. They show examples of less quiet regions in which eddy transport of q drives mean flow across q-contours as well. In this paper we extend these ideas to consider explicit, idealized models of wind-driven gyres. We treat a case in which repeated circulation of fluid about the gyre leads to a unique mean circulation. This contrasts the opposite extreme, 'meridional' view of water entering the ocean interior from the upper mixed layer, descending along isopycnal surfaces, taking perhaps half a turn about the gyre, then exiting. The real oceans no doubt involve something of both extremes.

Suppose the ocean is at rest, with density $\rho(z)$ prescribed. Shortly after the onset of a known wind-stress pattern the development of the planetary-scale ocean circulation can be calculated with linear wave theory (e.g., Anderson and Gill, 1975). The flow is initially barotropic (velocity independent of depth), and remains so until something occurs to break the zonal uniformity of vortex stretching throughout the water column. If there is a rigid boundary to the east, or if the stress-curl varies in the east-west direction, horizontal density gradients are created which propagate westward as planetary scale baroclinic Rossby waves. The arrival of successively higher vertical modes progressively brings the deep water to rest, so long as friction and eddy effects are locally weak. The vertically integrated north-south velocity is given by Sverdrup's relation as soon as barotropic adjustment has occurred. But the vertical distribution of this Sverdrup flow becomes increasingly singular as more baroclinic modes arrive; in a continuously stratified ocean the flow approaches a "delta-function jet" concentrated at the surface, while in a layered model the flow is eventually entirely in the uppermost layer. This result can be understood physically by realizing that in the linear model the potential vorticity is dominated by the β-effect so that all the geostrophic contours are open and can be traced back to either coastal boundaries or unforced, quiescent regions. Thus the no-motion boundary condition relevant to these regions is eventually communicated to all the interior flow with the result that the subsurface flow is "switched-off" by the baroclinic modes.

In this paper we show how simple nonlinear effects halt this vertical concentration of the wind circulation. Mesoscale eddies are the 'microscopic' phenomenon

that makes the nonlinear equilibration possible, but their detailed nature is relatively unimportant. In particular, they may be vanishingly weak. The result is a theory for inertial, wind-driven circulation in which there is near-conservation of potential vorticity, q, along streamlines ($q = Q(\psi, \rho)$, where ψ is the geostrophic streamfunction). The variation of potential vorticity across streamlines is determined by a development of the Prandtl-Batchelor theorem (Batchelor, 1956) given by Rhines and Young (1982) and summarized in Appendix A. The result is simply $\partial Q/\partial\psi = 0$ in many cases.

Isolation of the subsurface circulation in both the horizontal and the vertical occurs so that boundary conditions are prevented from affecting the interior potential vorticity of the gyres at lowest order. In the vertical sense this means that interior density surfaces, at levels deeper than that of direct influence of wind or surface cooling, obey free-flow equations. The only driving effects forcing these equations are weak averaged eddy—or molecular fluxes of potential vorticity, which tend to redistribute momentum principally in the vertical.

This means that we are omitting the processes that build up the basic thermocline, particularly the influx into the deep interior levels from the upper mixed layer: not totally ignoring them, but rather making them secondary in strength to the vertical flux of momentum by eddy stresses and subsuming them in the known basic stratification $\rho(z)$.

In the horizontal sense the closed streamlines of the gyre coincide with closed geostrophic contours, which are defined by $q = \text{const}$. Thus the influence of lateral boundary conditions cannot propagate into and influence the gyres, at least at high vertical mode numbers, since for weak signals the curves $q = \text{const}$. are characteristics of the wave equation.

The detailed discussion of western boundary intensification is deferred to a succeeding paper; some remarks can be found here, Section 6.

2. A two-layer model

We develop ideas with a layered quasigeostrophic calculation. The neglect of thermohaline processes is presumed in the use of the quasigeostrophic equations in which the basic buoyancy field is a prescribed function of z, the vertical coordinate only. These equations often reproduce qualitatively correct 'fast time-scale' phenomena even in cases where constant density surfaces penetrate from the upper boundary deep into the fluid (e.g., baroclinic instability in the atmosphere).

Each layer has mean depth H. The β-plane equations for the time-averaged, large-scale (Eulerian) flow are:

$$J(\psi_1, q_1) = W_0 - \nabla \cdot \mathbf{\Phi}_1 \tag{2.1a}$$

$$J(\psi_2, q_2) = -\nabla \cdot \mathbf{\Phi}_2 - D\,\nabla^2 \psi_2 \tag{2.1b}$$

where
$$q_1 = \beta y + F(\psi_2 - \psi_1) \tag{2.1c}$$
$$q_2 = \beta y + F(\psi_1 - \psi_2) \tag{2.1d}$$
$$F = f_o^2/g'H = L_\rho^{-2} = \{\text{Rossby radius of deformation}\}^{-2} \tag{2.1e}$$
$$W_o(x,y) = \nabla x\boldsymbol{\tau} \cdot \hat{\mathbf{z}}/\rho_o f_o H\,. \tag{2.1f}$$

The subscripts here denote the layer (upper = 1). ψ_i and q_i in the above are mean flow quantities. In the remainder of this article we will occasionally use an overbar to distinguish averaged variables. In most cases, however, when there is no risk of confusion, unadorned symbols denote mean quantities associated with the large-scale, wind-driven circulation. In (2.1) J is the Jacobian, $J(a,b) = \partial(a,b)/\partial(x,y)$, with respect to x and y (east and north, respectively). F is the Froude number, or the inverse square of the Rossby deformation scale, L_ρ. ψ_i are the streamfunctions and u_i the velocities. g' is the reduced gravity, $g\Delta\rho/\rho$. $\Delta\rho$ is the density step between adjacent layers. W_0 is the Ekman layer divergence, $\boldsymbol{\tau}$ the wind stress and $\hat{\mathbf{z}}$ a vertical unit vector. The relative vorticity of the mean flow is ignored because we are dealing with wind-gyre length scales, $L_m >> L_\rho$ where L_m is the length scale of the mean flow. The vertical vortex stretching component, which thus dominates q, is just f/h, where h is the thickness of a constant density layer. In the quasigeostrophic n-layer equations, the interface height is proportional to $\psi_i - \psi_{i-1}$. $D\,\nabla^2\psi_2$ is bottom drag on the lower layer.

Φ_i represents the effect of friction or geostrophic eddies. For example, with vertical friction, say an interfacial drag proportional to the velocity difference between the layers

(a)
$$\Phi_1 = R\,\nabla(\psi_1 - \psi_2)$$
$$\Phi_2 = R\,\nabla(\psi_2 - \psi_1)\,. \tag{2.2}$$

Alternatively, Φ may describe eddy flux of potential vorticity. With a prime denoting a fluctuation variable and the overbar a time-average,

(b) $$\Phi_i = \overline{q_i'\mathbf{u}_i'}\,.$$

In either case the principal effect is the vertical transport of horizontal momentum.[3]

3. Recall that $\overline{q'\mathbf{u}'}$ is dominated in baroclinic fields by this vertical (rather than lateral) momentum flux if typically,

$$\frac{f_o\,\overline{u'\eta'}}{H\,\dfrac{\partial}{\partial y}\,(\overline{u'v'})} >> 1$$

where η is the vertical perturbation height of an isopycnal surface due to the eddies. In terms of the lateral scale of eddies, L_e, and of the mean flow, L_m, this is

$$\frac{f_o^2 L_e^2}{N^2H^2}\;\frac{L_m}{L_e} >> 1\,.$$

Steady, frictionless, flow. Take the former prescription (*a*) for Φ and consider the lowest-order problem for small $R/\beta L_m$ (where L_m is the length scale of the circulation gyre). We will also assume $D = 0(R)$. Then (2.1) are:

$$J(\psi_1, \beta y + F\psi_2) = W_0 + 0(R)$$
$$J(\psi_2, \beta y + F\psi_1) = 0(R)\,. \tag{2.3}$$

We have used the fact that $J(\psi_2, \psi_2) = 0$, and neglected the $0(R)$ frictional terms.

One acceptable solution at this stage is

$$\psi_2 = 0$$
$$\psi_1 = -\beta^{-1}\int_x^\infty w_0 dx'\,.$$

In this article we will develop simple theories in unbounded oceans, rather than closed basins. This is why the upper limit in the above integral is ∞. The above is the traditional choice in which all the flow is confined to the upper layer. Provided w_0 is small enough (with weak winds) it is also the result of spinning up an inviscid ocean from rest. One might accept this as a reasonable solution were it not for the behavior as the vertical resolution (governed by n, the number of density layers) is increased. In a continuously stratified ocean confinement to the "uppermost" layer is the delta function catastrophe described earlier.

The general solution is found as follows: form the Sverdrup constraint by summing equations (2.2),

$$\psi_1 + \psi_2 = -\beta^{-1}\int_x^{x_E(y)} w_0 dx'$$
$$\equiv \psi_B(x,y) \tag{2.4}$$

ψ_B is the (known) transport streamfunction. In (2.4) $x_E(y)$ is the position of an eastern boundary where $\psi_1 = \psi_2 = 0$ or equivalently where w_0 vanishes. Although (2.2) are nonlinear they become linear by combining with (2.4):

$$J(\psi_1, \beta y + F\psi_B) = w_0 + 0(R)$$
$$J(\psi_2, \beta y + F\psi_B) = 0(R)\,. \tag{2.5}$$

Frequently $f_0^2 L_e^2/N^2H^2 \sim 1$ so the ratio of the vertical to lateral stress becomes just the scale separation parameter L_m/L_e between eddies and mean fields. If the η' fluctuations are primarily due to strong eddies, u_1, in the upper layer this ratio derived for the lower layer becomes:

$$\frac{f_0^2}{N^2}\,\frac{L_e^2}{H^2}\,\frac{L_m}{L_e}\,\frac{u_1}{u_2}$$

which is 'doubly' large when $u_1 >> u_2$ and $L_m >> L_e$ (Rhines and Holland, 1979, p. 320).

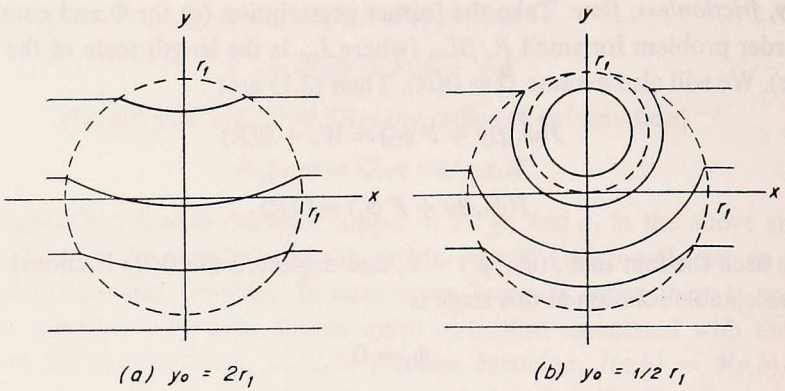

Figure 1. Contours of $\hat{q}_2$. The dashed circle is $r = r_1$ i.e., the bounding contour of the barotropic streamfunction. (a) The forcing is weak so $\hat{q}_2$ is dominated by βy and all the contours are open. (b) The forcing is stronger so there is a region of closed contours. The flow in this region is shielded from the eastern no-flux boundary condition which switches off the flow ($\psi_2 = 0$) in the open contour region.

This defines once and for all the geostrophic contours in the lower layer, they lie along isolines of the function

$$\hat{q}_2 = \beta y + F\psi_B$$

($\hat{q}_2$ also is the pattern of geostrophic contours that would exist in the upper layer under the assumption (2.3)).

These contours serve as characteristics for the first-order equation (2.5). The normal procedure, based on Rossby-wave group velocity arguments, is to integrate westward along $\hat{q}_2$ contours. The starting point is somewhere far to the east where $\nabla x\tau$ vanishes (and $\hat{q}_2 = \beta y$) or where an eastern boundary is encountered, see Figure 1. These zero values fill regions connected to the quiescent east by 'open' $\hat{q}_2$ contours. In the linear theory ψ_2 vanishes in this way.[4] For further discussion see Charney and Flierl (1980), Rhines and Holland (1979), Rooth *et al.* (1978).

Rooth *et al.* (1978) concluded that models with layered stratification cannot circulate at all, below the uppermost layer. This is not the case, for if ψ_B is sufficiently great, 'closed' $\hat{q}_2$-contours may exist beneath the regions of strongest Ekman divergence, where the slopes of $F\psi_B$ exceed β. These closed contours are completely isolated from eastern boundary conditions. The solution for the flow in such a region is given by

$$\psi_2 = A_2(\hat{q}_2) + 0(R) \tag{2.6}$$

for layer 2 where A_2 is, as yet, an undetermined function. Once A_2 is found, the

4. A nonlinear theory allowing finite excursions of the density surfaces has been discussed by Anderson and Killworth (1980).

upper-layer flow is given by:

$$\psi_1 = \psi_B(x,y) - \psi_2 .$$

The full potential vorticity functions are

$$\begin{aligned} q_1 &= \hat{q}_2 - 2F\,\psi_1 = \hat{q}_2 + 2FA_2(\hat{q}_2) - 2F\,\psi_B \\ q_2 &= \hat{q}_2 - 2F\,\psi_2 = \hat{q}_2 - 2FA_2(\hat{q}_2) . \end{aligned} \tag{2.7}$$

Notice that $\Sigma q_i = 2\beta y$; the contributions from the tilted interfaces vanish in the vertically integrated potential vorticity. If ∇q should be reduced in one layer, therefore, it must increase in another.

Figure 1 shows the $\hat{q}_2$ contours produced by a particularly simple pattern of Ekman pumping:

$$w_0 = \begin{cases} -\alpha x & \text{if } r < r_1 \\ 0 & \text{if } r > r_1 \end{cases}$$

where $r^2 = x^2 + y^2$. The ensuing barotropic circulation given by (2.4) is:

$$\psi_B = \begin{cases} \dfrac{\alpha}{2\beta}(r_1^2 - x^2 - y^2) & \text{if } r < r_1 \\ 0 & \text{if } r > r_1 . \end{cases}$$

The $\hat{q}_2$ contours are circles or arcs of circles if $r < r_1$; outside this circle they are just βy contours:

$$\hat{q}_2 = \begin{cases} \dfrac{\alpha F}{2\beta}[r_1^2 + y_0^2 - x^2 - (y-y_0)^2] & \text{if } r < r_1 \\ \beta y & \text{if } r > r_1 \end{cases}$$

where

$$y_0 = \frac{\beta^2}{\alpha F} .$$

The $\hat{q}_2$ contours close only if the forcing is sufficiently strong; more precisely if:

$$r_1 > y_0$$

or equivalently:

$$\alpha r_1 > \beta^2/F .$$

It is important to note that the forcing, w_0, in the example above has been contrived so that the barotropic streamlines given by the Sverdrup balance (2.4) close "naturally," i.e., it is not necessary to append a western boundary layer. For simplicity the present discussion is confined to these "mid-ocean" gyres produced by forcing patterns which satisfy:

$$\int_{-\infty}^{\infty} w_0 \, dx' = 0 \, . \tag{2.8}$$

Determination of the flow about closed geostrophic contours when $R = D$. With realistically strong winds ($\partial\psi_B/\partial y > \beta$ somewhere) there will be regions with closed $\hat{q}_2$ contours. If R and D vanish identically the unknown function A_2 in (2.6) cannot be found by spinning the circulation up from rest. In fact, the flow would never become steady. The fluid has perfect memory for its initial potential vorticity and the region of closed characteristics "traps" the baroclinic modes, preventing outward radiation of transients (Young, 1981). This is apparently not a satisfactory closure.

It is important to realize that if the right-hand side of (2.1b) were identically zero, A_2 would be completely arbitrary; any choice would be an acceptable solution. The resolution of this difficulty is provided by the small (order R) right-hand side of (2.1b). It is the nonconservative processes neglected to obtain the approximate solution (2.6), which determine A_2.

A relation which clearly exposes the importance of the small nonconservative terms, and also determines A_2, is obtained by integrating the steady balance (2.1b) about the region within a closed geostrophic contour:

$$R \oint \left(\mathbf{u}_2 - \frac{1}{2} \mathbf{u}_1 \right) \cdot d\mathbf{s} = 0 \tag{2.9}$$

where $\mathbf{u}_i = \hat{\mathbf{z}} \times \nabla\psi_i$ and $d\mathbf{s}$ is a vector element tangent to the circuit $\hat{q}_2 = \text{const}$. For convenience we have assumed that R in (2.2) is equal to D in (2.1b). Note how the large advective term and the β-effect vanish identically, leaving only the contribution from the nonconservative terms. Equation (2.9) is equivalent to:

$$\oint \mathbf{u}_2 \cdot d\mathbf{s} = \frac{1}{3} \oint \mathbf{u}_B \cdot d\mathbf{s} \tag{2.10}$$

where $\mathbf{u}_B = \hat{\mathbf{z}} \times \nabla \psi_B$. These statements are true regardless of the size of R. The unique solution for small R is found by combining (2.6) and (2.10). Equation (2.6) gives

$$\begin{aligned} \oint \mathbf{u}_2 \cdot d\mathbf{s} &= \oint A_2'(\hat{q}_2) \nabla \hat{q}_2 \cdot \hat{\mathbf{n}} ds \\ &= A_2'(\hat{q}_2) \oint (F\mathbf{u}_B - \beta\mathbf{x}) \cdot d\mathbf{s} \end{aligned}$$

where the primes indicate differentiation, and $\hat{\mathbf{x}}$ is an eastward pointing unit vector. Applying (2.10) and $\oint \hat{\mathbf{x}} \cdot d\mathbf{s} = 0$ one has:

$$\frac{1}{3F} \oint \mathbf{u}_B \cdot d\mathbf{s} = A_2'(\hat{q}_2) \oint \mathbf{u}_B \cdot d\mathbf{s}$$

or

$$A_2' = \frac{1}{3F} \, .$$

Hence:

$$\psi_2 = \frac{1}{3F}\hat{q}_2 + \text{const.}$$

$$= \frac{1}{3}\psi_B + \frac{1}{3}\frac{\beta y}{F} + \text{const.} \qquad \text{(closed } \hat{q}_2 \text{ regions)} \tag{2.11}$$

and:

$$\psi_2 = 0(R/\beta L)\,\psi_1 << \psi_1 \qquad \text{(open } \hat{q}_2 \text{ regions).}$$

The constant is chosen so that ψ_2 vanishes at the periphery of the 'island' of closed geostrophic contours.

Finally

$$\psi_1 = \psi_B - \psi_2\,. \tag{2.12}$$

The complete solution at 0(1) [(2.4), (2.11), (2.12)] is independent of friction. The vertical structure is reminiscent of the quasigeostrophic flow in an f-plane cylinder where top and bottom rotate at different rates, in which the inviscid fluid interior takes up solid rotation with vorticity equal to the average of that of the top and bottom plates.

In Figure 2, we plot various fields for the previous example, $w_0 = -\alpha x$, $r \leqslant r_1$. The Sverdrup depth-integrated transport is a solid-body rotation about (0,0). The lower-layer flow,

$$\psi_2 = -\frac{\alpha}{6\beta}(x^2 + (y - y_0)^2) + \text{const.} \quad \text{(in closed } \hat{q}_2\text{)} \tag{2.13}$$

$$= \text{const.} \qquad \text{(elsewhere)}$$

vanishes outside the closed contour region, and is a solid body rotation about a center displaced poleward by a distance $y_0 = \beta^2/\alpha F$. The upper-layer flow (the difference between ψ_B and ψ_2) is comprised of two sets of arcs of circles about centers (0,0) and (0,$-1/2\,y_0$),

$$\psi_1 = -\frac{\alpha}{3\beta}\left(x^2 + \left(y + \frac{1}{2}y_0\right)^2\right) + \text{const.} \quad \text{(closed } \hat{q}_2\text{)}$$

$$\psi_1 = \psi_B \qquad \text{(elsewhere)} \tag{2.14}$$

The velocity and temperature profiles have a north-south asymmetry with the northeastward branch of upper-level flow suddenly broadening as it crosses the boundary of the deep gyre.

Flow about closed geostrophic contours when $R \neq D$. In the previous subsection we discussed the calculation of A_2 in (2.6) when $R = D$ in (2.1) and (2.2). This restriction was purely for convenience. When the interfacial and bottom drags are unequal it is still straightforward to apply the integral theorems. One finds

$$A_2' = \frac{R}{(2R+D)F}$$

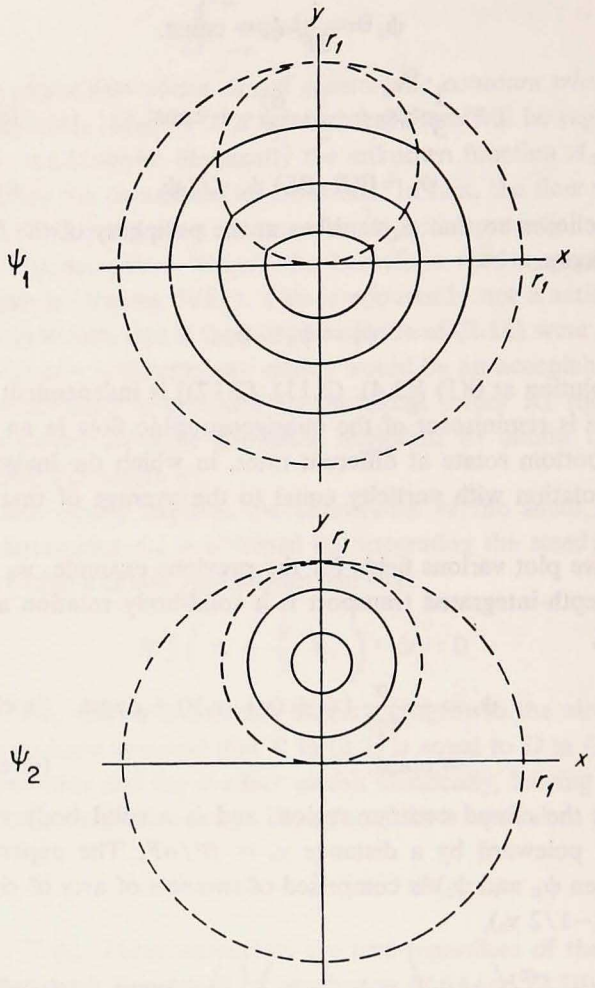

Figure 2. The streamfunctions given by (2.13) and (2.14) when $y_0 = \frac{1}{2} r_1$. The lower layer flow is confined to the region where the $\hat{q}_2$ contours close; see Figure 1(b).

so that the generalization of (2.11) is

$$\psi_2 = \frac{R}{(2R+D)}\left[\psi_B + \frac{\beta}{F} y\right] + (\text{const.}) \qquad (\text{inside closed } \hat{q}_2 \text{ contours})$$

The limits $R >> D$ and $D >> R$ are physically intuitive: in the first case the flow is essentially barotropic while in the second the strong bottom friction prevents the establishment of lower layer flows, even in the closed $\hat{q}_2$ regions.

In view of subsequent developments it is instructive to calculate the lower layer potential vorticity in the closed $\hat{q}_2$ regions:

$$q_2 = \beta y + F(\psi_1 - \psi_2)$$
$$= \hat{q}_2 - 2F\,\psi_2 + \text{const.}$$
$$= \left(\frac{D}{2R+D}\right)\hat{q}_2 + \text{const.} \qquad (2.15)$$

In the limit $D << R$ the potential vorticity becomes uniform. This is perhaps the simplest concrete example of the rather abstract arguments presented by Rhines and Young (1982): when the dissipation is equivalent to lateral diffusion of potential vorticity, the potential vorticity becomes uniform inside closed geostrophic contours. Equation (2.15) is particularly instructive because it shows the limitations of these homogenization arguments: arbitrary vertical stress does not homogenize potential vorticity. Only vertical stress equivalent to lateral diffusion of potential vorticity works.

3. A three-layer model

Despite its simplicity the two-layer model illustrates all the physical processes we wish to emphasize in this note:

(i) The production of closed geostrophic contours in the lower layer if the forcing is sufficiently strong.
(ii) The nonuniqueness of the flow in these closed regions if dissipation is entirely neglected.
(iii) The selection of a unique solution by the weak dissipation.
(iv) The calculation of this flow using the geostrophic contour integrals.
(v) The homogenization of potential vorticity within the closed contours when the dissipation is lateral potential vorticity diffusion.

In addition the two-layer model exhibits some features of the actual subtropical wind-driven gyres, namely a tight subsurface circulation shifted poleward relative to the broader surface flow. It would be interesting to explore the two-layer model further (for example, by relaxing the quasigeostrophic approximation and using a model such as that of Veronis, 1973). Instead we intend to discuss the shape of the gyre more thoroughly by increasing the vertical resolution.

The simplest model with increased vertical resolution is of course the three-layer model. A significant new feature of this model is the vertical isolation of the middle layer: it is not directly forced by Ekman pumping nor does it feel bottom drag. It is in regions like this, where the eddy flux of potential vorticity is likely to be the dominant dissipative process, that one expects to see potential vorticity homogenization.

The three-layer quasigeostrophic equations are:

$$J(\psi_1, q_1) = w_0 - \nabla \cdot \boldsymbol{\Phi}_1$$

$$J(\psi_2, q_2) = -\nabla \cdot \Phi_2 \tag{3.1}$$
$$J(\psi_3, q_3) = -\nabla \cdot \Phi_3 - D\nabla^2 \psi_3$$

where the potential vorticities are:

$$q_1 = \beta y + F(\psi_2 - \psi_1)$$
$$q_2 = \beta y + F(\psi_1 - 2\psi_2 + \psi_3) \tag{3.2}$$
$$q_3 = \beta y + F(\psi_2 - \psi_3)\,.$$

For simplicity we assume that the mean layer depths and density jumps are equal. If Φ_i is due to interfacial friction then:

$$\Phi_1 = R\nabla(\psi_1 - \psi_2)$$
$$\Phi_2 = R\nabla(2\psi_2 - \psi_1 - \psi_3) \tag{3.3}$$
$$\Phi_3 = R\nabla(\psi_3 - \psi_2)\,.$$

As in the previous section we can calculate the barotropic mode immediately by summing (3.1 a,b,c) and neglecting the bottom drag (the nonlinear and interfacial friction terms cancel):

$$\psi_1 + \psi_2 + \psi_3 = -\beta^{-1}\int_x^{x_E(y)} w_0 dx' \equiv \psi_B(x,y)\,. \tag{3.4}$$

When this is inserted in (3.1b) a linear equation:

$$J(\psi_2, \beta y + F\psi_B) = 0(R)$$

is obtained. Notice that as in Section 2 this linear equation determines the shape of the geostrophic contours once and for all, but not the functional dependence of q_2 and ψ_2 on $\hat{q}_2 = \beta y + F\psi_B$. It is significant that here, and in the two-layer model, the reshaping of the geostrophic contours is done by the barotropic mode, ψ_B. We write the general solution

$$\psi_2 = A_2(\hat{q}_2) + 0(R)$$
$$\hat{q}_2 = \beta y + F\psi_B \tag{3.5}$$

and from it solve for the lowest layer, from (3.1c) and (3.2c):

$$\psi_3 = A_3(\hat{q}_3) + 0(R)$$
$$\hat{q}_3 = \beta y + FA_2(\hat{q}_2)\,. \tag{3.6}$$

A_3 is a second undetermined function. A_2 and A_3 are now calculated using the integral method of Section 2; for simplicity we again take $R = D$. One has in the middle layer:

$$\oint \left(\mathbf{u}_2 - \frac{1}{2}(\mathbf{u}_1 + \mathbf{u}_3) \right) \cdot d\mathbf{s} = 0$$

from integrating (3.1b); on application of (3.4),

$$\oint \mathbf{u}_2 \cdot d\mathbf{s} = \frac{1}{3} \oint \mathbf{u}_B \cdot d\mathbf{s} \tag{3.7}$$

as before. The analogous circulation balance in layer 3 gives (recall $R = D$):

$$\oint \mathbf{u}_3 \cdot d\mathbf{s} = \frac{1}{2} \oint \mathbf{u}_2 \cdot d\mathbf{s} \,. \tag{3.8}$$

Combining (3.5) and (3.7) gives as before:

$$\begin{aligned} \psi_2 &= \frac{1}{3}\left(\psi_B + \frac{\beta y}{F} \right) + \text{const.} \qquad \text{(closed } \hat{q}_2\text{)} \\ &= 0(R/\beta L)\, \psi_1 \qquad \text{(elsewhere)} \,. \end{aligned} \tag{3.9}$$

The constant is set so that ψ_2 vanishes at the edge of the closed contour region. Now layer 3 is solved in like fashion. Equations (3.6) and (3.9) lead to:

$$\hat{q}_3 = \frac{1}{3} F \psi_B + \frac{4}{3} \beta y \tag{3.10a}$$

while (3.8) and (3.9) give:

$$\oint \mathbf{u}_3 \cdot d\mathbf{s} = \frac{1}{6} \oint \mathbf{u}_B \cdot d\mathbf{s} \,. \tag{3.10b}$$

Hence (3.6) combined with (3.10b) gives

$$\begin{aligned} \psi_3 &= \frac{1}{6}\, \psi_B + \frac{2}{3}\, \frac{\beta y}{F} + \text{const.} \qquad \text{(closed } \hat{q}_3\text{)} \\ &= 0(R/\beta L)\, \psi_2 \qquad \text{(elsewhere)} \,. \end{aligned} \tag{3.11}$$

Finally

$$\psi_1 = \psi_B - \psi_2 - \psi_3 \quad . \tag{3.12}$$

The region of closed $\hat{q}_3$ is smaller than, and properly contained in, the region of closed $\hat{q}_2$ contours (see Fig. 3). If the forcing is sufficiently weak, the $\hat{q}_2$ contours may close while all the $\hat{q}_3$ contours remain open. In this case the wind-driven flow is confined to the upper two layers while the lowest layer is motionless. The complete 0(1) solution [(3.9), (3.11), (3.12)] is independent of friction and obeys a simple "Couette" numerology, in which the average circulation in the jth layer of the velocity about $\hat{q}_i$ is the average of that above and below (Fig. 4).

Expulsion of potential vorticity gradients. Quite a general feature emerges when the full potential vorticity is calculated. Because:

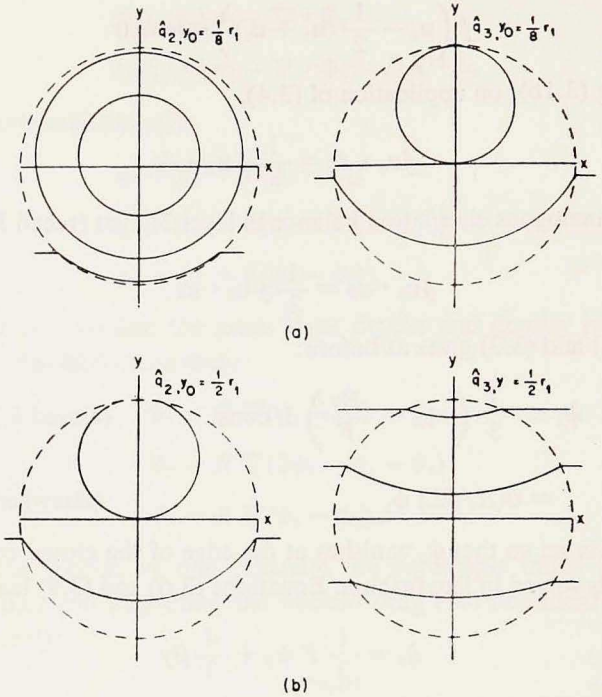

Figure 3. Contours of $\hat{q}_2$ from (3.5) and $\hat{q}_3$ from (3.10a). (a) Strong forcing. The forcing is strong enough to produce both closed $\hat{q}_2$ and closed $\hat{q}_3$ contours. The subsurface flow is confined to the region of closed contours. (b) Weaker forcing. The $\hat{q}_2$ contours are closed but all the $\hat{q}_3$ contours are open. Consequently there is no flow in the deepest layer.

$$q_2 = \hat{q}_2 - 3F\,\psi_2$$

(3.5), (3.9) yield

$$q_2 = \beta y + F\,\psi_B - 3F\left(\frac{1}{3}\,\psi_B + \frac{1}{3}\,\frac{\beta y}{F}\right) + \text{const.}$$

$$= \text{const.}$$

within the gyre. Without explicitly using that theory we have recovered the result of Rhines and Young (1982), that potential vorticity tends to homogenize in planetary gyres, on interior density layers. They give several proofs appropriate to a variety of assumptions about the flux Φ of potential vorticity by mesoscale eddies or friction. A review of these arguments is given in Appendix A.

The physical content of the idea is quite simple. The integral potential vorticity balance obtained by integrating the conservation equation over the region within a closed contour (which may be a contour of constant ψ or q) involves no advection of q by the mean Eulerian flow. If the flow is statistically steady the net flux $\oint \Phi \cdot \hat{\mathbf{n}}\, ds$ of q across the mean streamline must then vanish. Since there is a strong

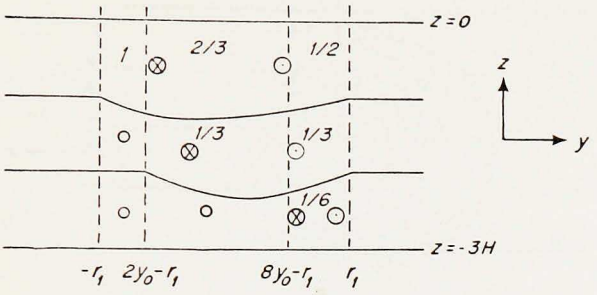

Figure 4. A schematic meridional section through the three-layer gyre. The numbers indicated the fraction of the Sverdrup transport carried by each layer. Note that each nonzero number is the average of those above and below.

tendency toward down-gradient q-fluxes on interior density layers of a large gyre, and since the bounding contour has a constant q, ∇q itself must vanish if the flux Φ does. Support for the idea comes from recent numerical models (Holland, 1982) and from ocean observations; see McDowell *et al.* (1982).

Calculation of the value of q_2 inside the closed contours. The constant value of q_2 inside the closed geostrophic contours is determined by requiring that $\psi_2 = 0$ on the outermost closed contour. From (3.9) and Figure 1 it then follows that

$$\psi_2 = \frac{1}{3}\left(\psi_B + \frac{\beta}{F}\, y\right) - \frac{1}{3}\,\frac{\beta}{F}\, r_1$$

since

$$\hat{q}_2 = \beta y + F\,\psi_B = \beta r_1 \quad \text{on this contour. Thus}$$

$$q_2 = \hat{q}_2 - 3F\,\psi_2$$

$$= \beta r_1 = \text{value of } \beta y \text{ at the most northerly point in the gyre.}$$

Character of the solution. The flow patterns are plotted in Figure 6 using the simple ψ_B pattern in Section 2, corresponding to a dipole of vertical velocity forcing $w_0 = -\alpha x$, or a wind-stress pattern like $\tau = (xy, 0)$ inside a circle of radius r_1. The streamlines again consist of arcs of circles:

$$\psi_2 = -\left(\frac{\alpha}{6\beta}\right)(x^2 + (y - y_0)^2) + (\text{const.}) \qquad (\text{closed } \hat{q}_2) \qquad (3.13a)$$

$$y_0 = \beta^2/\alpha F$$

$$\psi_3 = -\left(\frac{\alpha}{12\beta}\right)(x^2 + (y - 4y_0)^2) + (\text{const.}) \qquad (\text{closed } \hat{q}_3) \qquad (3.13b)$$

$$\psi_1 = \psi_B - \psi_2 - \psi_3 \qquad (3.13c)$$

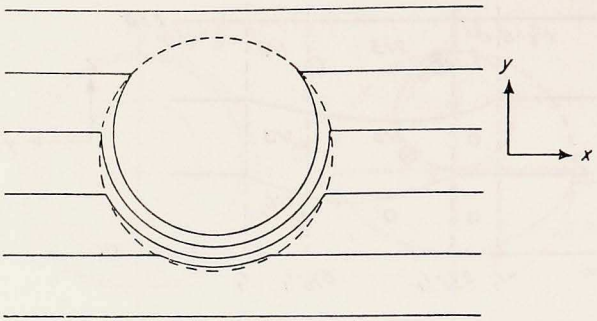

Figure 5. The potential vorticity in the middle layer, q_2. There is a large region of homogeneous q within which is the wind-driven flow. There are steep q-gradients as one passes out of the wind gyre.

$$= -\left(\frac{\alpha}{3\beta}\right)\left(x^2 + \left(y + \frac{1}{2}\, y_0 \right)^2 \right) + (\text{const.}) \qquad (\text{closed } \hat{q}_3, \text{ open } \hat{q}_2)$$

$$= -\left(\frac{\alpha}{4\beta}\right)(x^2 + (y + 2y_0)^2) + (\text{const.}) \qquad (\text{closed } \hat{q}_3, \text{ closed } \hat{q}_2)\,.$$

The center of the gyre in layer 2 is a distance $y_0 = \beta^2/\alpha F$ poleward of the center of ψ_B, the barotropic gyre, while the deepest, smallest gyre (layer 3) is displaced a distance $4y_0$ poleward of the center of ψ_B regardless of the choice of parameters (for equal mean layer depths, H). This skewed shape is a key feature of the theory, following simply from the constancy of q in the layer 2. As the figure indicates, the constancy of f/h_2 requires a poleward thickening of the isopycnal surfaces. Since the density surfaces are bowl-shaped, this thickening is created by a poleward shift of each deeper bowl relative to the one above. Equivalently, we may visualize the contours of $\hat{q}_2 = \beta y + F\,\psi_B$ as being the height contours of the surface ψ_B after tipping through an angle β/F. The gyre center is inevitably displaced poleward of the center of ψ_B.

An anticyclonic gyre thus develops a steep poleward boundary (and a cyclonic gyre an abrupt boundary on the side facing the equator). The plot of q_2 (Fig. 5) exhibits this property. Also evident are 'fringes' surrounding the gyre in which one interface is sloping, the layer above is moving, and yet the layer below cannot. Because of the weak stress exerted from above there develops in these regions of open q_2 contours a weak $0(R)$ flow. On the west side of the gyre this flow reaches far ($0(R^{-1})$) to the west, while on the east side a viscous boundary layer develops. Further discussion of $0(R)$ corrections is found in Appendix B.

4. Solution for the mean circulation of a turbulent 3-layer ocean

Instead of laminar interfacial friction and steady flow (choice (a) in (2.2)) sup-

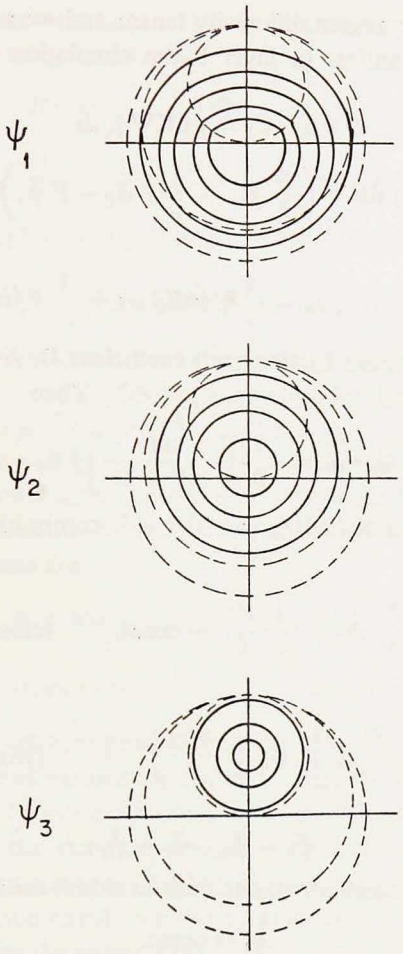

Figure 6. The streamfunctions ψ_1, ψ_2 and ψ_3 from (3.13) with $y_0 = 1/8$. Note the poleward shift of the gyre center as one moves downward. The outer dashed circle is $x^2 + y^2 = r_1^2$. The inner dashed circles are the outermost closed $\hat{q}_2$ and $\hat{q}_3$ contours.

pose we have a turbulent ocean, with eddy-induced stresses acting on the Eulerian mean circulation (choice (b) in (2.2)). As we discuss above (or in Rhines and Young (1982)), the sign of $\Phi \cdot \nabla q$ is negative on density layers free of external forces, providing that a scale separation exists between eddies and mean flow. Layer 2 of the model thus has uniform potential vorticity in regions of flow. Under these same conditions

$$\Phi_i = \overline{q' \mathbf{u}'}$$

$$= -\kappa_{ij} \partial \bar{q} / \partial x_j$$

where $\mathbf{K} = \kappa_{ij}$ is the Lagrangian diffusivity tensor and we temporarily use overbars to distinguish mean quantities. In layer 3 the circulation balance in (3.10) then becomes

$$D \oint \bar{\mathbf{u}}_3 \cdot d\mathbf{s} = \oint \hat{\mathbf{n}}\mathbf{K}\nabla\bar{q}_3 \, ds$$

$$= \oint \hat{\mathbf{n}}\mathbf{K}\nabla\left(\frac{4}{3}\beta y + \frac{1}{3}F\bar{\psi}_B - F\bar{\psi}_3\right) ds$$

or

$$\oint \hat{\mathbf{n}}\,(D + \mathbf{K}F)\,\nabla\psi_3 \, ds = \frac{4}{3}\beta \oint \hat{\mathbf{n}}\mathbf{K}\bar{\mathbf{y}} \, ds + \frac{1}{3}F \oint \hat{\mathbf{n}}\mathbf{K}\,\nabla\psi_B \, ds \ .$$

Here we have left in a bottom friction with coefficient D. As a simple example take κ_{ij} to be isotropic, diagonal and uniform, $\kappa_{ij} = A\delta_{ij}$. Then

$$\oint \bar{\mathbf{u}}_3 \cdot d\mathbf{s} = \frac{1}{3}\left[\frac{AF}{AF + D}\right] \oint \bar{\mathbf{u}}_B \cdot d\mathbf{s}$$

which is the generalization of (3.10), to which it becomes identical when $A = D/F$. Hence

$$\bar{\psi}_2 = \frac{1}{3}\,\bar{\psi}_B + \frac{1}{3}\frac{\beta y}{F} + \text{const.} \qquad \text{(closed } \hat{q}_2\text{)}$$

as before, yet

$$\bar{\psi}_3 = \frac{1}{3}\left[\frac{AF}{AF + D}\right]\left(\bar{\psi}_B + \frac{4\beta y}{F}\right) \qquad \text{(closed } \hat{q}_3\text{)}$$

and

$$\bar{\psi}_1 = \bar{\psi}_B - \bar{\psi}_2 - \bar{\psi}_3 \ .$$

It is also instructive to calculate q; one finds in closed-contour regions

$$\bar{q}_2 = \text{const.}$$

$$\bar{q}_3 = \left[\frac{D}{AF + D}\right]\left(\frac{4}{3}\beta y + \frac{1}{3}F\bar{\psi}_B\right) + \text{(const.)}$$

$$= \left[\frac{D}{AF + D}\right]\hat{q}_3 + \text{(const.)} \ .$$

As in Section 2, $\bar{q}_3$ is uniform if $AF >> D$; this is to be expected from the general results of Rhines and Young (1982) since this inequality ensures that the dissipation in the lower layer is equivalent to lateral diffusion of potential vorticity. In the middle layer $\bar{q}_2$ is always uniform, as in Figure 5.

5. The continuously stratified model

In this section we will extend the results of Section 3 to a continuously stratified model. Our goal is to develop more intuition about the shape of the bowl which

contains the wind-driven circulation. With continuous stratification the mean, Boussinesq potential vorticity equation is

$$J(\psi,q) = -\nabla \cdot \mathbf{\Phi} + w_0(x,y)\delta(z)$$

$$q = \psi_{xx} + \psi_{yy} + \left(\frac{f_0^2}{N^2}\,\psi_z\right)_z + \beta y\,. \tag{5.1}$$

As before ψ is the streamfunction and N the Brunt-Väisälä frequency. The vertical velocity is

$$w = -f_0\, N^{-2}\, J(\psi,\, \psi_z)$$

and the density field associated with the wind-driven flow is

$$\rho = \rho_0 \left\{ 1 - g^{-1} \int_0^z N^2 dz' - f_0 g^{-1}\, \psi_z \right\}$$

where g is the gravitational acceleration, ρ_0 the average density, N the buoyancy frequency and ψ_z the perturbation due to the wind-driven flow.

The boundary conditions are

$$w = w_0(x,y) \qquad \text{at } z = 0 \tag{5.2}$$

and

$$\psi,\, \psi_z \to 0 \qquad \text{as } z \to -\infty \tag{5.3}$$

where w_0 is the Ekman velocity produced by the wind stress curl. Suppose for the moment that the wind-curl vanishes north of $y = L_y$ and has zero integral in the east-west direction i.e., (2.8) (the condition for a 'mid-ocean' gyre). The first boundary condition, (5.2), is the standard condition applied at the base of the upper Ekman layer. The second condition, (5.3), comes from requiring that the perturbations due to the wind-driven circulation vanish in the deep water.

Now nondimensionalize the above using the following scalings

$$\psi = UL_y\, \psi_*$$

$$z = \left(\frac{f_0}{N_0}\right)\left(\frac{U}{\beta}\right)^{1/2} z_*$$

$$(x,y) = L_y(x_*,T_*)$$

$$w = Ww_* \tag{5.4}$$

where W is a typical vertical velocity scale forced by the wind curl. We will assume that the flow is in Sverdrup balance, $\beta v = f w_z$, so with the above estimate of the vertical scale one can express U in terms of the external parameters:

$$U = (N_0 W)^{2/3}\, \beta^{-1/3} \tag{5.5}$$

and so (5.4b) gives:

$$\text{(vertical length scale)} = f_0(N_0\beta)^{-2/3}\, W^{1/3}.$$

In (5.4) and (5.5), N_0 is a typical value of the Brunt-Väisälä frequency in the wind-driven part of the water column. The potential vorticity is (dropping the *'s):

$$\tilde{q} = \beta L_y(\epsilon^2 \nabla^2 \psi + (F\psi_z)_z + y)$$

where

$$F = N_0^2/N^2$$

$$\epsilon^2 = U/\beta L_y^2 \quad . \tag{5.6}$$

As before $\epsilon^2 << 1$, so that the relative vorticity is negligible in the interior. The density field is

$$\rho = \rho_0 \left\{ 1 - N_0^2 g^{-1} \left[\int^z F^{-1} dz' + \left(\frac{\beta L_y}{f_0} \right) \psi_z \right] \right\}.$$

This last relation shows that the quasigeostrophic relation is valid to the extent that $(\beta L_y/f_0)$ is small.

The most important part of (5.4) is the choice of $(f_0/N_0)\sqrt{U/\beta}$ as a vertical scale. This scale is determined by requiring that the deformation of the isopycnal surfaces create potential vorticity gradients comparable to the β-effect so that the geostrophic contours can close (Rhines and Holland, 1979).

Now suppose that the wind-driven circulation lies between $z = -D(x,y)$ and $z = 0$; $D(x,y)$ is the "bowl" which vertically bounds the wind-driven flow. A primary goal of this section is to determine the unknown D in terms of w_0 and F. The potential vorticity is uniform on density surfaces within the bowl, (see Appendix A) so that

$$(F\psi_z)_z + y = \Upsilon(z) \qquad \text{if } -D < z < 0\,. \tag{5.7}$$

$\Upsilon(z)$ is the initially unknown value of the potential vorticity at the level z. Outside the bowl ψ vanishes so that

$$\psi = 0 \qquad \text{if } z < -D\,. \tag{5.8}$$

We will now solve (5.7) assuming that F is constant; because of (5.6) we can set $F = 1$ without loss of generality. The function $\Upsilon(z)$ is determined from the matching conditions at the outermost closed q-contour. Recall that in an anticyclonic gyre the three-layer model developed uniform potential vorticity, with the constant value being close to the value of planetary vorticity, $f_0 + \beta y$, at the poleward extremity of the barotropic gyre ($y = 1$ in the nondimensional units of this section). This suggests setting Υ equal to this extreme latitude here. We will justify this choice below. The solution of (5.7) which satisfies

$$\psi = \psi_z = 0 \qquad \text{on } z = -D$$

is then

$$\psi = \frac{1}{2}(z + D)^2\,(\Upsilon - y) \tag{5.9}$$

since Υ is a constant. For example if $\psi_B = 1 - x^2 - y^2$ (when $x^2 + y^2 < 1$), as in Section 2, then $\Upsilon = 1$. $D(x,y)$ is determined by applying the boundary condition (5.2). The vertical velocity is

$$w = \frac{1}{2}(z + D)^2 (\Upsilon - y) D_x \tag{5.10}$$

so that (5.2) implies

$$\frac{\partial D^3}{\partial x} = 6(\Upsilon - y)^{-1} w_E$$

or, since D vanishes at large x,

$$D^3 = 6(\Upsilon - y)^{-1} \psi_B \quad . \tag{5.11}$$

The above is the principal result of this section *viz.*, an expression for the depth of the wind-driven flow in terms of the forcing and other external parameters.

The full solution (5.9), (5.11), may be combined to give

$$\psi = \frac{1}{2}[z(\Upsilon - y)^{1/2} + (6\psi_B)^{1/3} (\Upsilon - y)^{1/6}]^2$$

where Υ is determined by the curve $\psi_B = 0$; Υ is the poleward-most value of y on this curve if $\psi_B > 0$, and the equatorward-most value if $\psi_B < 0$. In the above expression we have assumed that $\psi_B > 0$ so $\Upsilon - y > 0$.

The displacement of an isopycnal surface, η, in this solution is proportional to ψ_z,

$$\psi_z = (\Upsilon - y)(z + D) \tag{5.12}$$

and the isopycnals in Figure 7 are contours of $z + \left(\frac{\beta L_y}{f_0}\right)\psi_z$ with $\beta L_y / f_0 = \frac{1}{4}$.

The streamlines corresponding to (5.9) and (5.11) are surprisingly hard to visualize. For simplicity we shall use the by now familiar barotropic streamfunction:

$$\psi_B = \begin{cases} 1 - x^2 - y^2 & (\text{if } x^2 + y^2 < 1) \\ 0 & (\text{otherwise}) . \end{cases} \tag{5.13}$$

Since $y = 1$ is the most northerly point of this anticyclonic circulation we expect that:

$$\Upsilon = 1 .$$

The gyre is deepest at $(x = 0, y = 1)$ where

$$D = (12)^{1/3} = D_{\max}$$

from (5.11).

These continuously stratified models have vanishing velocity and density pertur-

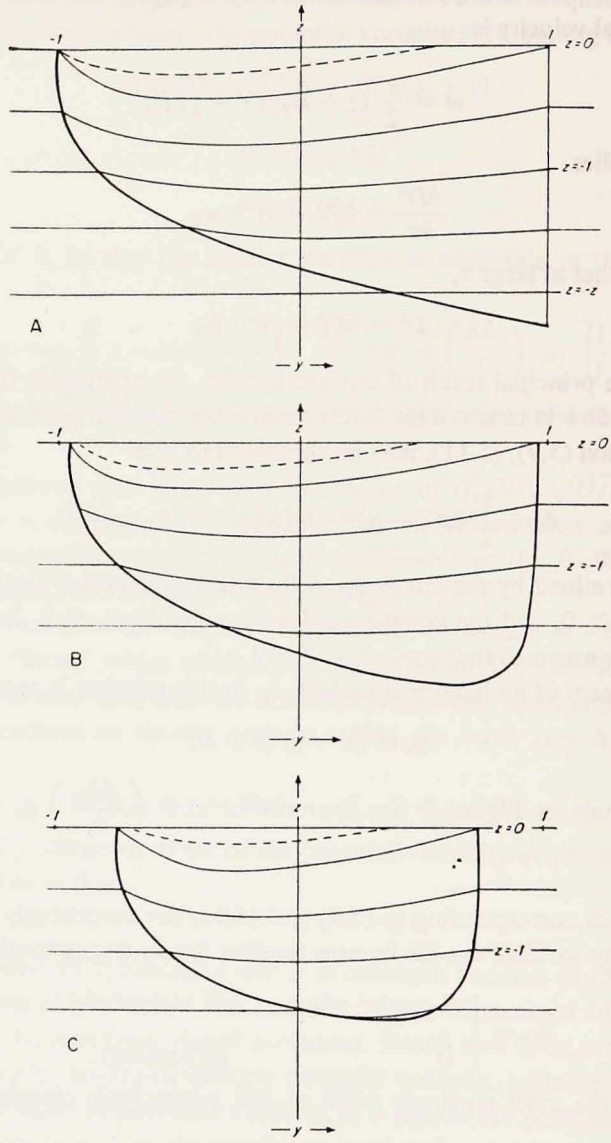

Figure 7. Three meridional sections through the gyre at $x = 0, \frac{1}{3}, \frac{2}{3}$ showing the density field $z + \left(\frac{\beta L_y}{f_0}\right)\psi_z$ computed from (5.12) with $(\beta L_y/f_0) = \frac{1}{4}$. The isopycnal slope is discontinuous at $z = -D(x,y)$ (shown as a heavy line in the figure). An additional contour (dashed) has been included near the surface to show the isopycnal intersections with $z = 0$.

bation as well as vanishing vertical velocity gradient at the rim of the gyre ($\psi = \psi_z = \nabla\psi_z = 0$ at $z = -D$). The solutions are smoother than with the layered models, which have vortex-sheet discontinuities of horizontal velocity. They exhibit, however, an interestingly abrupt poleward edge at the latitude of zero-wind-curl. [A wind profile more relevant to the oceans would have an extended line of vanishing curl where η is discontinuous. In such a case (say $\psi_B = \sin y \sin x$) the poleward front is long and deep.]

The northward horizontal velocity predicted here increases linearly with z, from a zero value at the base of the gyre. The eastward velocity is a quadratic in z, which may reverse with depth due to the skewed shape of the gyre. The hodograph of v against u spirals with depth to the right if the vertical velocity, w, is negative and conversely. w itself is quadratic in z.

The choice of Y *(i.e., the vertical variation of q), and the spin-up of the flow.* The form of (5.9) has q taking on the same constant value, Y, at each depth in the gyre. This requires some explanation, and some apology for a case in which this choice of Y(z) is incorrect.

To see how the gyre selects its potential vorticity, recall the arguments accompanying the three-layer model: if all the Sverdrup flow were initially confined to the upper layer, it would produce in the layer below a potential vorticity field $\hat{q}_2$ composed of βy plus the contribution of $f_0\eta/H$ due to the dish-shaped thermocline overhead, Figure 8a. In section, this is a 'dish' tipped up on a ramp. Supposing the flow to be strong enough to produce an island of closed geostrophic contours, any vertical flux of momentum (no matter how weak) will spin-up the flow in layer 2. As this occurs, the true potential vorticity q_2 descends as a plateau, Figure 8b. We know q_2 to be a constant, and this constant is reached when q_2 is tangent to $\hat{q}_2$ on the poleward side. Then flow has developed fully about all available geostrophic contours.

q_2 goes no further downward because it now has no impetus to and it has no more free paths: the eddy force causing this spin-up is proportional to $\overline{q'\mathbf{u}'}$, and we equate this to $-\mathbf{K}\,\nabla\bar{q}$. Suppose $\mathbf{K}$ is a constant diagonal tensor; then the eddy force is directed pseudo-westward about the contours in Figure 1. It accelerates the flow about the island until the mean state adjusts toward

$$\nabla\,\bar{q} = 0$$

so that the eddy forces vanish. The circulation thus incapacitates the force field, $-\mathbf{K}\,\nabla\bar{q}$, that created it, and henceforth rests in equilibrium.[5]

The source of the eddies that do this work is most likely to be instability of the initial flow, which occurs as a baroclinic instability if that flow is strong enough to

5. The eddy force does not go entirely into accelerating the flow, but also sets up the altered density field by a 'meridional' circulation. This greatly reduces the rate of spin-up of the deeper layers, as the Coriolis force acting on the great mass-field adjustment opposes the acceleration that creates it.

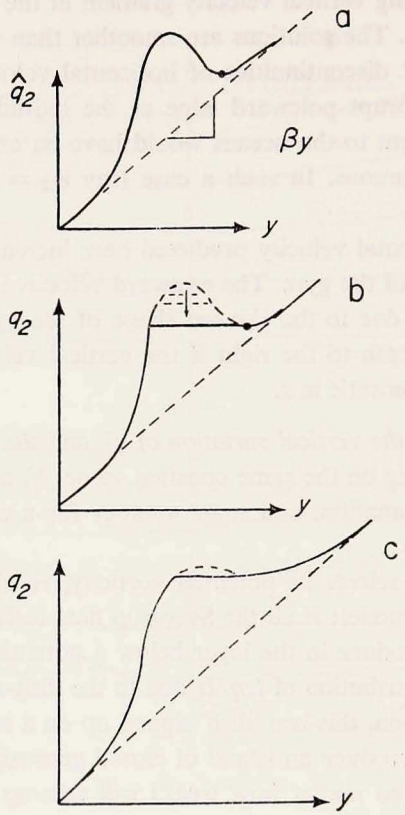

Figure 8. (a) A section showing $\hat{q}_2 = \beta_y + F\psi_B$ as a function of y. (b) A schematic of the evolution of q_2 from the initial state $\hat{q}_2$ in (a) to the final homogenized state. The constant value of q_2 is determined by the condition on the poleward boundary. (c) If ψ_B fails gradually to zero as $y \to \infty$, the poleward boundary of the homogeneous region does not coincide with the poleward boundary of the ψ_B pattern.

cause the potential vorticity gradient to reverse somewhere in the gyre. Indeed the appearance of closed $\hat{q}_2$ contours as the strength of the forcing is increased coincides with the first reversal of the northward potential vorticity gradient in the lower layer if one assumes that the flow is given by:

$$\psi_1 = \psi_B$$

$$\psi_2 = 0\,,$$

so that $q_2 = \hat{q}_2$. This observation provides an additional physical interpretation of the homogenization result: the flow develops in the subsurface layer so as to just cancel the change in sign of q_y. Thus the mean flows poleward of the gyre center, calculated using the potential vorticity homogenization argument, are marginally stable according to the Charney-Stern generalization of Rayleigh's theorem. Equator-

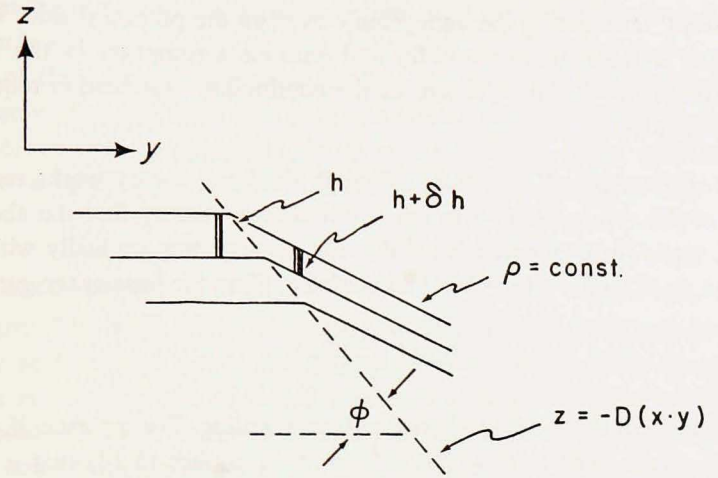

Figure 9. An illustration of the geometry accompanying (5.14). Unless the gyre boundary (the dashed line) is vertical, a discontinuity in slope of the isopycnals implies a discontinuity in the potential vorticity at $y = Y$.

ward of the gyre center the reversal of q_y in the upper layer provides for baroclinic instability.

Notice that if ψ_B decreases to zero quickly enough as one approaches $y = Y$, the final state (which lies tangent with the minimum of the original $\hat{q}_2$ curve) is nearly a ledge with q intersecting βy near the 'contact point' βY. This shows that, as the number of layers, n, of an n-layer model is increased, *(i) q tends to a ledge with a discontinuity on the equatorward side, and continuity on the poleward side* (for an anticyclone, conversely for a cyclone).

Now it follows simply that for q to be continuous at $y = Y$, *the gyre boundary must be vertical there.* [As Fig. 9 shows, the jump in f/h across the gyre boundary is simply

$$\frac{\delta q}{q} = -\frac{\delta h}{n} = \cot\phi \, \frac{\partial \eta}{\partial y} \tag{5.14}$$

where ϕ is the angle of repose of the boundary $z = -D(x,y)$. Therefore if $\delta q = 0$, $\phi = \frac{\pi}{2}$.]

Thus, the latitude of intersection of q with βy is independent of depth, and so Y is a constant, the potential vorticity of the gyre is a single constant[6] and there is

6. This uniform q has the dimensions of $Hf/(H + h')$, where H and h' are mean and perturbation layer thicknesses. The form used frequently, $\frac{f}{\rho_0}\frac{\partial \rho}{\partial z}$, differs in dimensions. In a nonuniform stratification our q is constant in the vertical whereas $\frac{f}{\rho_0}\frac{\partial \rho}{\partial z}$ varies like N^2.

a vertical 'front' terminating the anticyclonic gyre on the poleward side. We remark that all these features arose naturally and without assumption in the three-layer model, but the method of integration for the continuous stratification required these further arguments.[7]

Failures of the choice $\Upsilon = const.$ Although the layer theory works regardless of the nature of the winds, we find in the continuous-N^2 theory that the above choice $\Upsilon = \text{const.}$ leads to inconsistencies if ψ_B falls to zero too gradually with y: more exactly, if $(\partial \psi_B/\partial y)/\psi_B < (y - \Upsilon)^{-1}$ somewhere. Then the base of the gyre,

$$D = \left(\frac{6\,\psi_B}{\Upsilon - y}\right)^{1/3}$$

deepens somewhere south of $y = \Upsilon$ rather than shoaling. For instance, if $\psi_B \sim (y - \Upsilon)^2$ near $y = \Upsilon$, then $D \sim (y - \Upsilon)^{1/3}$ there. This implies (5.14) that q cannot be continuous, and our chain of reasoning is broken. It is easy to see (Fig. 8c) in the layered model how the point of vanishing ψ_B can become distant from the termination of the constant q region if ψ_B is slowly falling to zero with y in this way. (The appropriate changes in the theory for this case remain to be carried out.)

A singularity arises if ψ_B drops precipitously to zero. For example, if $\psi_B \sim (\Upsilon - y)^{1/2}$ near $y = \Upsilon$ then $D \sim (\Upsilon - y)^{-1/2}$ is singular at that point. This appears to be a physically consistent result which in the real fluid would be limited by the presence of the sea floor, or by eddy fluxes of q.

Realistic wind-stress patterns rarely suffer from either of these problems; for example a zonal wind-stress varying like $\sin y$ produces a pair of wind gyres antisymmetric about $y = 0$ with a vertical 'front' between them.

Density boundary conditions. The greatest difficulty in any of the vast set of 'stratified spin-up' problems is connected with the mixing and exchange of density near the fluid boundaries. In the layer models given earlier the wind-induced pumping at the surface involves homogeneous fluid, and standard Ekman theory suffices. The continuously stratified model requires more discussion, for the fluid at $z = 0$ is not isopycnal. The model described just above is valid if (i) we understand it to be the limit of an n-layer model as n becomes large *but* with $n < \left(\frac{NH}{fL}\right)\left(\frac{f}{(U\beta)^{1/2}}\right)$ (to insure that no out-cropping of isopycnals occurs at $z = 0$), *or* (ii) if we artificially prescribe the density of fluid at $z = 0$ in downwelling regions (as with forcing by injection of fluid rather than wind stress), *or* (iii) and perhaps most appealing, if we modify the theory by putting a single, thin, homogeneous layer to overlie the stratified fluid below. This last resolution might occur in an experiment where surface

7. The transition from the layered to continuous stratification has other interesting features. The resolution here assumes that the number of layers, $n \to \infty$, $R \to 0$ with $nR << 1$, where R is the drag coefficient between the layers.

stresses eventually mix the uppermost region, and the upper surface is insulating (rather than insolating).

In spite of these qualifications this β-plane theory is far closer to being a satisfactory solution than one finds with the same boundary stresses applied to an f-plane fluid. There, the linearly stratified spin-up solution breaks down quickly, as heavy fluid flows over light, unless molecular diffusion of density is very strong.

6. Discussion: dynamics

q-geometry. The wind-driven circulation is described here as a restructuring of the density surfaces and hence the dynamical environment from one of blocked geostrophic contours to one of closed geostrophic contours, along which flow can freely proceed. This can occur in a variety of initial-value problems as with flow burrowing down from the upper ocean or relaxing from the barotropic motion that follows a sudden onset of winds: but the result is always the same. The Sverdrup transport, which is fixed by the pattern of wind-curl, distributes itself with depth in such a way that ledges of uniform potential vorticity are built on the β-'hillside'. The communication of the flow vertically, across isopycnal surfaces, is carried out by mesoscale-eddy pressure drag, simply a generalization of Rossby-wave drag, that works against the ambient gradient of q. As the circulation reaches its final configuration, these q-gradients disappear inside the gyre, and hence the eddy forces drop away to nothing. Subsequently there is almost no eddy flux of potential vorticity, nor any perturbation potential vorticity.[8] The mean flow is then also marginally stable according to the generalized Rayleigh criterion, on the poleward side of the gyre, and strongly unstable on the equatorward side.

At the large scales of the 'mid-ocean' gyres described here the relative vorticity is slight, so that $q \cong \frac{f}{\rho_0}\frac{\partial \rho}{\partial z}$ can be calculated from hydrographic data alone. The β-effect is cancelled if isopycnal layers thicken poleward at just the right rate. To do so, the gyre center at each deeper level must be displaced poleward (for anticyclones). This is a familiar property of the observed wind gyres (Montgomery and Pollack, 1942). It is interesting that the barotropic mode, ψ_B, plays the dominant role in determining the deep geostrophic contours.

The constant value selected for q is not a simple average of the neighboring environment, but is skewed to the poleward side (for anticyclones), conversely for cyclones. The vertical variation of fdp/dz follows that of N^2. The scale depth of the wind gyre, $\frac{f}{N}\left(\frac{U}{\beta}\right)^{1/2}$, arises simply by requiring that $\frac{f^2}{N^2}\, u_{zz} \sim \beta$ so as to ensure that the deformation of the density surfaces can cancel the β-effect.

8. This warns against the conclusion that eddies must be unimportant if their average q-transport is observed to be weak.

Boundary currents. The absence of strong sources and sinks of q below the mixed layer determines this structure (eddies are sources of $\bar{q}$ in the interior, but they are not strong enough to violate $\bar{u} \cdot \nabla \bar{q} = 0$ over planetary scales). The models here avoid boundary currents by the choice $\int_{-\infty}^{\infty} w_0 dx = 0$. However if we insert a rigid meridional boundary in the center of the model gyres given here, we find far less need to construct dissipative western boundary currents: the interior streamlines are nearly geostrophic contours, so the fluid must have the same value of q when it exits the boundary region, as when it entered. In contrast to the traditional one-layer ocean theory we expect *inertial* boundary layers to dominate upon these deep density surfaces. Inner frictional layers must exist in most prescriptions for the coastal boundary conditions, but their net effect may be small.

In the homogeneous-fluid circulation theory we find that fluid columns lose potential vorticity in mid-ocean by the wind, and must regain it by frictional flux in the boundary current. In a vertically integrated sense, this must still be true, but we relegate the changes to near-surface layers, and perhaps to benthic boundary layers. In the interior regions, where the potential vorticity is uniform, there is no compelling reason to introduce a frictional flux in the western boundary. We should also be willing to allow the possibility that, far from the coast, bottom topographic wave-drag, interior bottom friction, or lateral eddy q-transport each could balance the net wind-stress curl, rather than invoking frictional or pressure-drag processes concentrated at the western boundary.

Outcrops and renewal. Fluid enters the interior from the upper mixed layer and proceeds along a sort of stochastic helix, circulating in the gyre while descending. The whole sense of the theory presented here is that this helix is tightly pitched, with fluid going round enough times to expel gradients of q before eventually exiting (by eddy scattering at the gyre boundary or by flow out the base of the gyre). Thus, we do not ignore the outcropping of density surfaces, but consider for the expulsion theorem only the circulation contours which encircle no strong q-sources on a potential density horizon.

The ratio of the rate of recirculation about the wind-gyre, to the rate of renewal from the surface is thus a key measure of the strength of the gyre, and of the process of expulsion of potential vorticity gradients that determine its mean structure. Chemical tracer data may be particularly useful in observing the vertical penetration of the gyre from above; indeed tritium analyses (Jenkins, 1980; Fine *et al.*, 1981; Sarmiento, 1982) have recently been used in this way. Figure 10, from Jenkins' paper is particularly revealing of the renewal process. At the *Panulirus* site, near Bermuda (32N, 64W) the vertical profile of tritium shows that, indeed significant renewal from the surface has occurred since the early 1960's, down well below the base of the wind-gyre. By contrast, the helium-3 nearly vanishes at levels

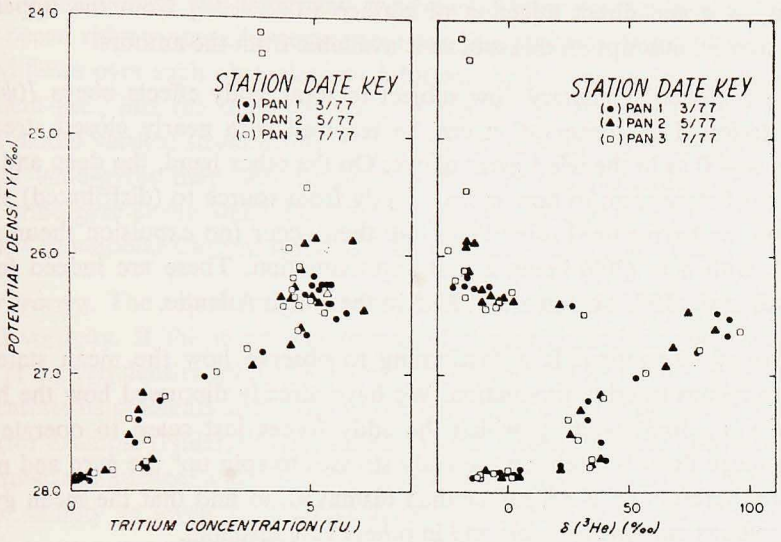

Figure 10. (a) Tritium concentration *vs.* potential density. There is a significant concentration of tritium down to the bottom of the wind gyre ($\sigma_\theta = 27.5$ or roughly 1000 m). (b) ^{3}He *vs.* potential density. ^{3}He is the decay product of tritium. The absence of ^{3}He above $\sigma_\theta = 26.5$ (roughly 400 m) indicates that this water above this level is frequently by contact with the atmosphere. From Jenkins (1980).

above a potential density, σ_θ, of 26.5. This is characteristic of very rapid renewal of these upper levels (helium-3 is removed efficiently at the sea surface, but develops below by tritium decay).

These profiles suggest that what we term 'interior' density layers lie below $\sigma_\theta = 26.5$ corresponding perhaps to the deepest level of winter convection in the intensely recirculating parts of gyre.

A problem for the near future will be to construct a theory allowing the surfacing of isopycnals in a layered model. It will take on some of the aspects of Veronis' (1973) two-layer model of the world ocean.

We have avoided considering the creation of the thermocline, itself, which is studied in parallel with the wind circulation by Welander (1971), Needler (1972). There are intersections with the present work (for example, thermocline similarity theory often proceeds by assuming q to be constant on density surfaces, whereas we show q to evolve in this direction in gyres, but with important discontinuities of q at the gyre boundary). Although we assume the basic stratification as given, the circulations are unique functions of the wind-stress distribution, unlike the non-unique families of solutions that arise from the more difficult thermocline theory.

The rate of expulsion of q-gradients during spin-up of the gyre has not been analyzed here. It is important to consideration of the competition between 'homog-

enization' of q and direct injection of surface values of q from the upper mixed layer. A new manuscript on this subject is available from the authors.

Deep circulation. Planetary flow subject to weak eddy effects obeys $J(\psi,q) = 0$ in the interior. This conservation can be resolved with nearly closed streamlines, $\nabla q = 0$, $\psi \neq 0$ as in the wind gyres above. On the other hand, the deep and abyssal circulations below seem to flow more directly from source to (distributed) sink. We expect that well-structured q-gradients can then occur (no expulsion theorem being possible), with $q = Q(\psi)$ being a first approximation. These are indeed found by McDowell *et al.* (1982) below $\sigma_\Theta = 27.5$ in the North Atlantic.

Stability of circulation. It is fascinating to observe how the mean state of the wind-gyre relates to eddy production. We have already discussed how the homogenized gyre is a limit point at which the eddy forces just cease to operate on the Eulerian mean flow. We rely on the eddy stresses to spin up[9] the gyre and maintain it. We are therefore relieved, rather than dismayed, to find that the mean gyres are in some regions marginally stable and in others very unstable.

The homogenization of q might make it seem that fluid particles could move freely about a σ_Θ surface, the β-effect having been cancelled. But to the contrary the flow in these homogenized regions is determined by the 'outer' density surfaces into which the q-gradients have been concentrated (in the sense that in the homogenized regions ψ is determined by inverting an equation of the form $(F\,\psi_z)_z = q - \beta(y - y_0)$ subject to boundary conditions at the outer density surfaces). Just as in Eady's instability problem, the motion in the near-boundary sheets of potential vorticity determines the interior flow perturbations. This might suggest a way of reducing the numerical computations necessary to model the circulation on a computer. It will be interesting to study the perturbation problem both with a view to instability, and to the behavior of baroclinic Rossby waves encountering the major abrupt change in $\nabla\bar{q}$ and in current.

Topography. Thinking primarily of the shallow wind-gyres, we have not mentioned bottom topography. A level bottom was included in the layered model; in the continuously stratified model (5.11) must be simply rewritten to satisfy the Sverdrup relation wherever the predicted D exceeds H. q may be affected in the deepest layers through bottom-friction drag (as in the three-layer model). Topographic roughness, to a first approximation, merely accentuates the down-gradient mixing of the large-scale q, and is in this sense already present in the theory. It and other kinds of eddy enstrophy dissipation can replace western boundary drag as the

9. The vertical transport of momentum by eddy pressure drag may be thought of as a spin-up mechanism in which $A\bar{u}_{zz} = \kappa \nabla \bar{q} \sim \frac{f^2}{N^2}\bar{u}_{zz}$ determines the effective vertical viscosity, A. Thus $A \sim \frac{f^2}{N^2}\kappa$ is large $\sim 10^5 \text{cm}^2\text{sec}^{-1}$ typically, κ being the Lagrangian *lateral* diffusivity.

principal opposition to the integrated wind-curl. Major topographic features like the mid-ocean ridge system, however, pose another problem. It may be shown that westward flows over such obstacles are deformed only to a height $\sim (f/N)\sqrt{U/\beta}$ above them (i.e., just the thickness scale of the gyres). Eastward flows, however, generate modal vertical structure which penetrates through the water column. Even the upper wind-gyres may thus be deformed. The deep penetration of the anticyclonic wind gyre in the South Pacific might in part be due to interaction with the Antarctic Circumpolar Current where it flows over the East Pacific Rise.

Other tracers. The expulsion property works for other conservative tracers than potential vorticity. If the input and output of a geochemical tracer is sufficiently gradual at a given density level, the action of the gyre will be to homogenize it, and to concentrate its gradients at the rim of the gyre. This effect is quite visible in some tracers (for example (Niiler, 1981), salinity in the North Atlantic above the strong Mediterranean influence, and also tritium at some levels) yet less so in others (for example, salinity at levels of Mediterranean input, and dissolved oxygen at the levels of strong consumption). Study of the advection-diffusion properties of tracers in these gyres will be rewarding.

β-spiral. In constructing a dynamically based method of determining the reference level for geostrophic velocity computation from density data, Stommel and Schott (1977) find a local best-fit tangent-plane to the geostrophic contours, q = constant. Their results suggest a level of no motion near 750 m at 28N, 36W in the eastern North Atlantic. Consistent with our theory, however, they find the gradients of q vanish above about $\sigma_\Theta = 27.0$. Of course the β-spiral method must fail in these homogenized regions. However their method succeeds on the basis of well-determined geostrophic contours below the strongly flowing wind gyre. Were there no density-driven flows below the wind gyre, we would have predicted a level of no motion ($\psi \to 0$) at levels where ∇q becomes nonzero, and this is not a bad approximation to the actual state of affairs. In the more intense circulation nearer the Gulf Stream the gyre base does seem much deeper, as in the models, and regions of homogeneous q reach to deeper σ_Θ levels.

Other ocean observations. The β-spiral method may be regarded as locally fitting tangent planes to the surfaces $q(x,y,\sigma_\Theta)$, to determine the direction of flow. A complementary approach, initiated by Behringer (1972) is to develop maps of $q \cong f\partial\sigma_\Theta/\partial z$ from hydrographic data for entire ocean basins. The resulting charts of geostrophic contours are useful in several ways: as idealized flow paths at each density horizon; in showing 'expelled' regions where gyre activity is strong; in suggesting where eddy activity or interaction with surface or bottom will force flow across q-contours; in diagnosing boundary-current dynamics by viewing the q-distribution of fluid exiting to mid-ocean; in providing the mean field for calculation

of wave propagation, and, in showing regions where flow instability is possible, due to reversals of the gradient of q.

Charts of q for the North Atlantic (McDowell *et al.*, 1982) show that despite the outcropping of density surfaces and the presence of western boundary currents, much of the subtropical wind gyre contains uniform potential vorticity in the density range $\sigma_\Theta = 26.5\text{-}27.3$. Below, the q-contours show well-defined gradients which may indicate the paths of flow of various source-sink flows like Labrador Sea Water and Mediterranean Water.

Not all methods of observing the general circulation show close agreement with one another. Moored current meters are particularly susceptible to small-scale gyres induced by eddies and rough topography, which may mask the large-scale circulation. In order to circumvent the problem clusters of five moorings each were deployed as a part of the POLYMODE program. The 12-month records, augmented by site moorings and hydrography, show a substantial northward flow of the water below 500 m depth near 28N, 48W and 27N, 41W (Keffer and Niiler, 1980). These are sites on either side of the Mid-Atlantic Ridge. Above 500 m, the general sense of the circulation agrees with the usual picture of the wind gyre but in the deeper water this northward flow is not easy to reconcile with the generally east-west strike of the mid-depth geostrophic contours. Neither the dynamical nor the observational reconstruction of flows beneath the wind gyres is in particularly good order.

Numerical models. The sequence of ocean models being developed by Dr. Holland is particularly well suited to exploring q-expulsion and the structure of the wind gyre. Recent experiments (Holland, 1982) with three density layers in a 4000 × 4000 km basin (200 × 200 grid) show, in the intermediate density layer, regions roughly 3000 km × 1500 km in size with uniform potential vorticity (both instantaneously and in the mean), (Fig. 11). The potential vorticity is homogeneous to within a few percent, even in the presence of western boundary currents. These experiments give us the opportunity to watch the detail of the expulsion process, and to include inertial-gyre effects not present in the detailed circulation models given here.

The recent model of Bleck and Boudra (1981) allows density surfaces to outcrop at the sea surface. The potential vorticity, in agreement with this theory, forms 'islands' with closed contours and, in the deeper layers remote from direct forcing, large areas of uniform potential vorticity.

Acknowledgments. Funding was provided by the National Science Foundation grant OCE-77-25692, and by fellowships from the J. S. Guggenheim Foundation and Christ's College, Cambridge. We are grateful to George Batchelor and the Dept. of Applied Mathematics and Theoretical Physics, Cambridge University, for their hospitality during this sabbatical. This is contribution number 5107 from the Woods Hole Oceanographic Institution.

We thank W. R. Holland for discussions on the relation between the numerical models and theory, and Henry Stommel and Larry Armi for showing us their recent data from the 'β triangle'; the 'β-spiral' provided a stimulating complement to this theory.

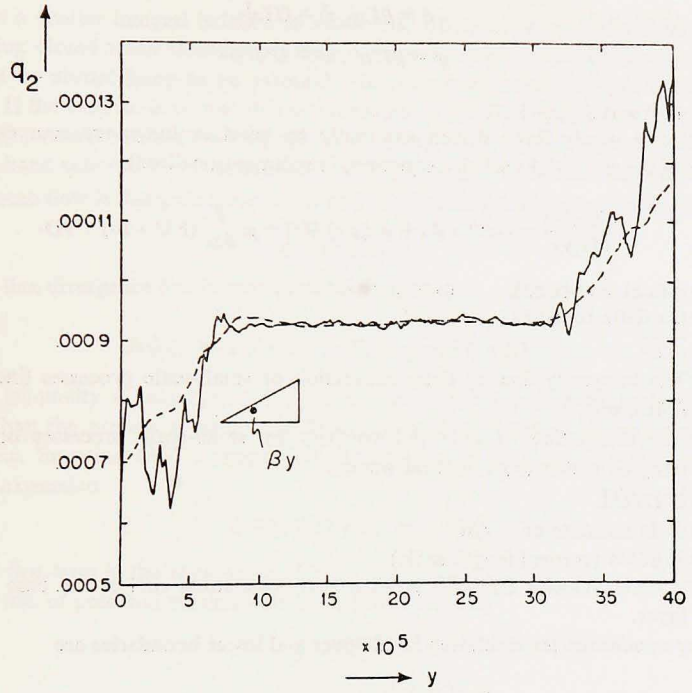

Figure 11. A meridional section, showing potential vorticity as a function of latitude, through Holland's three-layer eddy resolving general circulation model. The solid line is the instantaneous q_2 field while the dashed curve is an 1,800-day average. The large region of uniform q is striking.

We are indebted to L. V. Worthington for lending us over the years his insight and good humor. He has characterized the North Atlantic as being dominated by recirculating gyres rather than ins and outs. We hope he finds these mathematical gyres, conceived in the same spirit, to be appealing. As to the role of eddies we apologize to him for their necessity, but at least they are weak in their interaction with the fully developed gyres. One day, during his rounds as Chairman, LVW peered over our shoulders at his North Atlantic Atlas, seized on an isolated salinity contour drawn about a single station, and said, "that's real, an eddy: a blemish on the face of an otherwise perfect ocean." He remains a laminar animal.

APPENDIX

A. A general discussion of potential vorticity homogenization

The following discussion follows Rhines and Young (1982) closely and has been included here for the sake of completeness.

We will be primarily concerned with the interaction between the mean flow, characterized by velocity and horizontal length scales $\bar{U}$ and $\bar{L}$ and vertical length scale given by (5.5b), and mesoscale eddies, characterized by U' and L'. These scales are used to define nondimensional variables, denoted temporarily by *,

$$\bar{q} = \beta L q_*, \ \bar{\psi} = UL\bar{\psi}_*$$

$$q' = \beta L' q'_*, \ \psi' = U'L'\psi'_*$$

where $q = \bar{q} + q'$ and $\psi = \bar{\psi} + \psi'$.

For statistically steady flows driven externally by wind or buoyancy sources we write the time-average of the potential vorticity equation, (nondimensionalized):

$$\frac{\partial(\bar{\psi}_*, \bar{q}_*)}{\partial(x,y)} = -\epsilon \nabla \cdot \mathbf{\Phi}_* + w_0(x,y)\,\delta(z) + \mu \frac{\partial}{\partial z_*}(F \nabla \cdot \mathbf{B}_*) + \nu \mathbf{D}_* \qquad \text{(A1)}$$

where $q_* = \bar{q}_*(\mathbf{x},z) + q'_*(\mathbf{x},z,t)$, $\quad \psi_* = \bar{\psi}_* + \psi'_* \ldots$.

$\delta(z)$ = the delta function

$\mathbf{\Phi}_* = \overline{q_*' u_*'}$

$\mathbf{B}_*$ = The buoyancy flux by deep convection or small-scale processes (including density diffusion)

$\mathbf{D}_*$ = The dissipation of potential vorticity by small-scale processes other than geostrophic eddies (e.g., internal waves).

$\epsilon = U'L'/\bar{U}\bar{L}$

ν = scale estimate of $\quad /\beta\bar{U}$

$\mu = 1/\beta\bar{U} \times$ (vertical length scale)

w_0 = vertical velocity ($xf_0/\beta U$) produced by wind-stress curl at the base of the Ekman layer.

The boundary conditions for insulating level upper and lower boundaries are

$$\frac{D}{Dt}\left(\frac{\partial \bar{\psi}_*}{\partial z}\right) = 0 \qquad \text{on } z = 0, -H$$

and

$$\frac{\partial \bar{\psi}_*}{\partial s} = 0$$

on a free-slip lateral boundary (s being the displacement along the boundary). $\partial\bar{\psi}/\partial z$ is proportional to perturbation density. Note the wind stress forcing at the upper boundary has been shown explicitly on the RHS of (A1) using the mathematical artifice of a delta function (Bretherton, 1966).

The equations allow significant interaction of the upper boundary with the deep interior only by vortex stretching, but not by advection from the surface. A necessary condition for their validity is

$$\frac{L}{a} << 1$$

where L is the lateral scale of a gyre streamline and a is the earth's radius. It is just to this same degree that the mid-latitude β-plane is valid.

In analyzing a particular ocean circulation model Holland and Rhines (1980) found it useful to study the vorticity balance integrated over an area bounded by a time-averaged streamline. In the uppermost layer, the circulation of the wind-stress, $\rho_0 f_0 \iint w_0 dxdy = \oint \boldsymbol{\tau} \cdot d\mathbf{s}$, was balanced by a combination of lateral momentum flux by eddies (to adjacent gyre streamlines) and downward momentum flux, which drove a deep circulation. In the deep layer the effect of this downward eddy flux was balanced principally by bottom friction. The procedure is analogous to zonal averaging in simplified atmospheric 'channel' models.

Here we use a similar integral balance to prove that, if gyres exist, (defined by curves ψ or q = const. being closed upon themselves) then *q must in many cases be uniform within the gyres.* There is an abrupt jump to an external q-field as one passes through the boundary of the wind gyre. If the exterior is at rest, this external field is just the 'ramp', $q = \beta y$.

The assumptions made in the following derivation are:

(i) The right-hand side of (A1) is small i.e., $z < 0$ and $\epsilon,\nu,\mu << 1$. Thus as a first approximation the mean flow is dissipationless and $\bar{q}$ and $\bar{\psi}$ contours are almost coincident:

$$\bar{q} = Q(\bar{\psi},z)\,. \tag{A2}$$

(ii) The eddy flux divergence has intermediate strength i.e.,

$$J(\bar{\psi},\bar{q}) >> \epsilon\nabla\cdot\mathbf{\Phi} >> \nu\mathbf{D},\ \mu\frac{\partial}{\partial z}(F\nabla\cdot\mathbf{B})\,. \tag{A3}$$

The first inequality is assumption (i); the second inequality implies that the eddies are stronger than the process subsumed in **D** and **B** such as internal waves, penetrative convection, etc. Equation (A3) suggests that the solution of (A1) can be obtained as a perturbation expansion

$$\bar{q} = Q(\psi,z) + \epsilon q_1 + \ldots \tag{A4}$$

where the first term in the expansion is (A2).

(iii) The eddy flux of potential vorticity can be approximated by

$$\mathbf{\Phi}_i = \overline{u'_i q'}$$

$$= -\kappa_{ij}\frac{\partial\bar{q}}{\partial x_j} + 0(\gamma) \tag{A5}$$

where:

$$\gamma = \frac{\text{eddy particle excursion}}{\text{length scale of mean flow}} << 1$$

κ_{ij} = Lagrangian diffusivity of fluid particles

= the ensemble average $<u_i x_j>$ where x_i and u_i are the displacement and velocity of a particle.

The parameterization (A5) has been discussed in detail elsewhere (Rhines and Holland, 1979).

(iv) The symmetric part of κ_{ij}:

$$S_{ij} = \frac{1}{2}(\kappa_{ij} + \kappa_{ji}) \tag{A6}$$

is positive definite i.e.,

$$S_{ij}\,a_i\,a_j > 0 \tag{A7}$$

for all nonzero vectors a_i, everywhere in the flow. Note that the above is guaranteed if $S_{ij} = A(\mathbf{x})\,\delta_{ij}$. In general, however, the condition is:

$$S_{11}\,S_{22} > S_{12}^2\,.$$

This condition on the symmetric part of κ_{ij} is related to the assertion that in a turbulent fluid a cloud of particles expands about its center of mass, rather than contracts. Since:

$$\overline{\mathbf{u}'q'}\cdot\nabla\bar{q} = -\kappa_{ij}\frac{\partial\bar{q}}{\partial x_i}\frac{\partial\bar{q}}{\partial x_j} + 0(\gamma)$$

$$= -S_{ij}\frac{\partial\bar{q}}{\partial x_i}\frac{\partial\bar{q}}{\partial x_j} + 0(\gamma) \tag{A8}$$

(A7) amounts to an assertion that the eddy flux of potential vorticity is downgradient everywhere. It will become apparent in the course of the derivation below that this last assumption is stronger than necessary; we will only require that (A7) apply in an integrated sense.

Begin by integrating (A1) over the area enclosed by a ψ-contour. This area will be denoted by A_ψ and its boundary by B_ψ. The large advective term on the left-hand side vanishes identically leaving an integral balance between eddies, dissipation and heating:

$$-\epsilon \oint_{B_\psi} \Phi \cdot \hat{\mathbf{n}}\, ds + \nu \iint_{A_\psi} \mathbf{D}\, d^2a + \mu \oint_{B_\psi} (F\mathbf{B})_z \cdot \hat{\mathbf{n}}\, ds = 0 \tag{A9}$$

(we take $z \neq 0$, so there is no contribution from the Ekman pumping $w_0(x,y)$). Note that (A9) is an exact result, not relying on assumptions (i)-(iv) above.

Now from (A3) and (A5), (A9) reduces to:

$$\oint_{B_\psi} \kappa_{ij} \frac{\partial \bar{q}}{\partial x_j} n_i\, ds = 0\left(\frac{\nu,\mu}{\epsilon}\right) << 1$$

and substituting the perturbation expansion (A4) into the above together with:

$$n = \nabla\psi/|\nabla\psi| = \text{unit normal to } B_\psi$$

gives:

$$\frac{\partial Q}{\partial \psi} \oint_{B_\psi} S_{ij}\, \psi_{,i}\, \psi_{,j} \frac{ds}{|\nabla\psi|} = 0\left(\frac{\nu,\mu}{\epsilon}\right)^1. \tag{A10}$$

Assumption (iv) then ensures that the line integral is nonzero so that to leading order the potential vorticity is uniform. It is clear from (A10) that (A7) is stronger than necessary; S_{ij} need only be positive definite in the integrated sense required by assuming that the line integral in (A10) is nonzero. Since this notion is rather ill defined we thought it best to make the strong assumption (A7) from the outset.

B. 0(R) Corrections

Although some of the properties described here (like homogenization of q) may be fairly general, the specific model circulations have assumed that the vertical transport of momentum by eddies or by analogous friction, R, to be small, $R/\beta L_m << 1$. This allowed $q = Q(\psi,\rho)$ to be the first approximation to the dynamics and caused the flow to vanish on open geostrophic contours, at lowest order.

Without calculating any detailed higher corrections we outline here what their nature should be. The spinning circulation terminates at the surface $z = -D(x,y)$ where the velocity (u,v,w) vanishes, but the gradients (u_z,v_z) are discontinuous. Taking friction to model the eddy q-transport, there is thus a stress imbalance $R(u_z,v_z)$ which will tend weakly to accelerate the water beneath the gyre. On the western sides of the gyre the correction field will radiate westward along $q = \beta y$ contours. To the east the correction field will tend to form a boundary current along the rim of the 'bowl'.

Notice that the interior homogenized field has $\psi_{zz} = \beta(y - y_0)$, hence the frictional vorticity term $R\nabla^2\psi_{zz}$ vanishes; there is no correction field in the gyre interior. But there is a weak, spatially uniform eastward force there (for an anticyclone, conversely for a cyclone) corresponding to the quadratic $u(z)$ profile. The opposition to this force must come from motions generated below, which will tend to be weak, but could produce locally stronger velocities in thin boundary layers on the deep eastern sides of the gyre.

REFERENCES

Anderson, D. and A. E. Gill. 1975. Spin-up of a stratified ocean with application to upwelling. Deep-Sea Res., *22,* 583–596.

Anderson, D. and P. Killworth. 1980. Nonlinear propagation of long Rossby waves. Deep-Sea Res., *26,* 1033–1050.

Batchelor, G. K. 1956. Steady, laminar flow with closed streamlines at large Reynolds number. J. Fluid Mech., *1,* 177–190.

Behringer, D. W. 1972. Investigations of large-scale oceanic circulation using hydrographic data. Ph.D. thesis, University of California, San Diego.

Bleck, R. and D. B. Boudra. 1981. Initial testing of a numerical ocean circulation model using a hybrid (quasi-isopycnic) vertical coordinate. J. Phys. Oceanogr., *11,* 755–770.

Bretherton, F. P. 1966. Baroclinic instability and the short wavelength cut-off in terms of potential vorticity. Quart. J. Roy. Meteorol. Soc., *92,* 335–345.

Charney, J. and G. Flierl. 1980. Oceanic analogues of large-scale atmosphere motions, *in* Evolution of Physical Oceanography, B. Warren and C. Wunsch, eds., MIT Press, Cambridge, 504–549.

Coats, D. A. 1981. An estimate of absolute geostrophic velocity from the density field in the Northeastern Pacific Ocean. J. Geophys. Res., (submitted).

Eady, E. T. 1949. Long waves and cyclone waves. Tellus, *1,* 33–52.

Fine, R. A., J. L. Reid and H. G. Östlund. 1981. Circulation of tritium in the Pacific Ocean. J. Phys. Oceanogr., *11,* 3–14.

Holland, W. R. 1982. Regions of uniform potential vorticity in an ocean circulation model with mesoscale resolution, (in preparation).

Holland, W. R. and P. B. Rhines. 1980. An example of eddy induced ocean circulation. J. Phys. Oceanogr., *10,* 1010–1031.

Jenkins, W. J. 1980. Tritium and ^{3}He in the Sargasso Sea. J. Mar. Res., *38,* 533–569.

Keffer, T. and P. P. Niiler. 1980. The vertical structure of observed and geostrophically derived mean flow and heat and salt eddy convergence in the sub-tropical North Atlantic, Ch. III. Ph.D. dissertation, Oregon State University.

McDowell, S., P. B. Rhines and T. Keffer. 1982. Geostrophic contours for the North Atlantic, (in preparation).

Montgomery, R. and M. J. Pollack. 1942. Sigma-*t* surfaces in the Atlantic Ocean. J. Mar. Res., *5,* 20–27.

Needler, G. 1972. Thermocline models with arbitrary barotropic flow. Deep-Sea Res., *18,* 895–903.

Niiler, P. 1981. General circulation of the oceans, *in* Oceanography—the Next 50 Years, P. Brewer, ed., Proceedings of a symposium at W.H.O.I.

Pedlosky, J. 1979. Geophysical Fluid Dynamics, Springer-Verlag, Berlin.

Rhines, P. B. and W. R. Holland. 1979. A theoretical discussion of eddy-induced circulation. Dyn. Atmos. Oceans, *3,* 285–325.

Rhines, P. B. and W. R. Young. 1982. Potential vorticity homogenization in planetary gyres. J. Fluid Mech., (in press).

Rooth, C., H. Stommel and G. Veronis. 1978. On motion in steady layered geostrophic models. J. Oceanogr. Soc. Japan, *34,* 265–267.

Sarmiento, J. 1981. Personal communication.

Stommel, H. and F. Schott. 1977. The β-spiral and the determination of the absolute velocity field from oceanographic station data. Deep-Sea Res., *24,* 325–329.

Veronis, G. 1973. Model of world ocean circulation, I. Wind-driven two-layer. J. Mar. Res., *31,* 228–288.

Welander, P. 1971. Some exact solutions to the equations describing an ideal-fluid thermocline. J. Mar. Res., *29*, 60–68.

Young, W. R. 1981. The vertical structure of the wind-driven circulation. Ph.D. dissertation, W.H.O.I./M.I.T. program in Oceanography.

Young, W. R. and P. B. Rhines. 1982. A theory of the wind-driven circulation II. Circulation models and western boundary layers. J. Mar. Res., *40*, (in press).

Received: *23 September, 1981*; revised: *11 February, 1982.*